Solar energy conversion via hot electron internal photoemission in metallic nanostructures: Efficiency estimates

Andrew J. Leenheer, Prineha Narang, Nathan S. Lewis, and Harry A. Atwater

Citation: Journal of Applied Physics **115**, 134301 (2014); doi: 10.1063/1.4870040
View online: http://dx.doi.org/10.1063/1.4870040
View Table of Contents: http://scitation.aip.org/content/aip/journal/jap/115/13?ver=pdfcov
Published by the AIP Publishing

Solar energy conversion via hot electron internal photoemission in metallic nanostructures: Efficiency estimates

Andrew J. Leenheer,[1,2] Prineha Narang,[1,2] Nathan S. Lewis,[3,2] and Harry A. Atwater[1,2,a)]
[1]*Thomas J. Watson Laboratories of Applied Physics, California Institute of Technology, Pasadena, California 91125, USA*
[2]*Joint Center for Artificial Photosynthesis, Pasadena, California 91125, USA*
[3]*Division of Chemistry and Chemical Engineering, California Institute of Technology, Pasadena, California 91125, USA*

(Received 31 October 2013; accepted 15 February 2014; published online 1 April 2014)

Collection of hot electrons generated by the efficient absorption of light in metallic nanostructures, in contact with semiconductor substrates can provide a basis for the construction of solar energy-conversion devices. Herein, we evaluate theoretically the energy-conversion efficiency of systems that rely on internal photoemission processes at metal-semiconductor Schottky-barrier diodes. In this theory, the current-voltage characteristics are given by the internal photoemission yield as well as by the thermionic dark current over a varied-energy barrier height. The Fowler model, in all cases, predicts solar energy-conversion efficiencies of $<1\%$ for such systems. However, relaxation of the assumptions regarding constraints on the escape cone and momentum conservation at the interface yields solar energy-conversion efficiencies as high as 1%–10%, under some assumed (albeit optimistic) operating conditions. Under these conditions, the energy-conversion efficiency is mainly limited by the thermionic dark current, the distribution of hot electron energies, and hot-electron momentum considerations. © *2014 AIP Publishing LLC*. [http://dx.doi.org/10.1063/1.4870040]

I. INTRODUCTION

The energy-conversion efficiencies of record-setting *pn*-junction photovoltaics are rapidly approaching the theoretical single-bandgap Shockley-Queisser limit of 32% under unconcentrated sunlight.[1] Multi-junction solar cells (that still operate within the Shockley-Queisser limitations for each absorber and junction) can provide much higher efficiencies partly by reducing the amount of sub-bandgap light lost, but such devices also have much higher costs than single-bandgap devices due to the need to produce multiple high-purity semiconductor materials to capture the incident light and convert it into a collected electrical current. Another possible device architecture considered here consists of a single band gap semiconductor homojunction or heterojunction device used in combination with a metal-semiconductor Schottky junction formed from that same light absorber. In such an approach, in addition to collection of above band-gap carriers generated in the semiconductor (again subject to the Shockley-Queisser limit), the metal would additionally serve to generate "hot" electron-hole pairs in the metal which would then be emitted into the semiconductor and collected as an additional photocurrent. The process of hot carrier internal photoemission (IPE) from the metal to the semiconductor over a tuneable Schottky barrier has therefore been proposed as a possible solar energy conversion device formation strategy.[2,3] This metal-absorber device structure (similar in some ways to a dye-sensitized solar cell) could therefore provide an interesting device integration possibility when placed optically behind a single-junction solar cell, serving to increase the overall efficiency of the whole system by virtue of the presence of this second capture and conversion system in the overall device structure. Though referred to as "hot electron" or "hot hole" emission/capture, we emphasize that the device physics are different from "hot carrier" solar cells.[4] Such hot carrier metal/semiconductor device structures could, in principle, be beneficially used in solid-state[2,5–10] or photoelectrochemical[11–16] systems to collect photons having energies lower than the energy band gap of a semiconductor, in essence, serving as the second junction in a tandem structure but not requiring necessarily a second pure semiconductor light absorber as in a conventional tandem cell arrangement.

Plasmonic structures have been demonstrated to provide highly efficient light scattering and trapping elements, in some cases, providing enhancements in solar energy conversion.[17] In the context of hot-electron devices, the large extinction cross-section at a surface plasmon resonance enables very thin films of nanostructures to absorb a significant fraction of the solar spectrum.[18] The collective plasmon oscillation may also play a role in increasing the photoemission yield,[19,20] though the details of the hot-carrier dynamics after surface plasmon decay are still under study. At the small dimensions of plasmonic structures, the effects of electron scattering at surfaces strongly modifies the yield even in the semiclassical IPE model.[21,22]

Herein, we present an analysis of the efficiency limits for energy conversion via IPE, capturing the key optical and electronic processes in such devices. Section II presents the current-voltage characteristics and energy-conversion efficiency based on simple Fowler theory and thermionic emission; Section III reviews the three-step model of internal photoemission and describes explicitly the inherent assumptions of Fowler theory; Section IV refines the yield including the effect of phonon scattering and thin-film enhancement; Section V presents example calculations of the limiting

a)E-mail: haa@caltech.edu

efficiency under various assumptions; and Section VI discusses the application of these approaches to plasmonic structures. Previous estimates of the IPE yield and energy-conversion efficiency of such systems have used simple Fowler theory and/or have used a simplified treatment of the carrier dynamics, with a recent study by White and Catchpole consequently calculating a maximum best case solar energy-conversion efficiency of 8% for such systems.[3] In contrast, we describe the situation in which realistic assumptions are made and the carrier dynamics are fully treated. Our most generous efficiency estimates agree with previous "absolute upper-limit" efficiency values,[2,3] which assumed that the momentum requirements at the interface governing emission (the hot electron escape cone) can be relaxed for nanostructures. However, our more in-depth analysis shows that even for nanostructures of dimensions on the order of 20 nm, the practically obtainable efficiency is lowered by orders of magnitude due to the limiting effects of the hot electron mean free path in conjunction with the requirement of a critical momentum normal to the interface. The lowered efficiency limits calculated herein thus serve as a more realistic framework for establishing the expected efficiencies, design parameters, and performance characteristics, of an actual energy-conversion system based on metallic hot-carrier internal photoemission.

II. INTERNAL PHOTOEMISSION AND EFFICIENCY

Fowler developed the basic theory of photon-induced emission of electrons from metals in the early 20th century.[23] Though refinements have been made,[22,24,25] the simple Fowler equation has proven to be in accord with experimental data for the internal photoemission yield[26] in both magnitude and spectral behaviour

$$Y_{Fow}(\hbar\omega) \approx \frac{1}{8E_F}\frac{(\hbar\omega - \phi_b)^2}{\hbar\omega}, \tag{1}$$

where ħ is the reduced Planck constant, ω is the incident light frequency, φ_b is the barrier height (in units of energy), and E_F is the Fermi energy of the emitter, with the value of E_F describing the curvature of the conduction band in momentum space (Figure 1(a)) (This treatment assumes a 1-dimensional problem as shown in Figure 1(a), though the results should not differ significantly for the 3-dimensional case.) The Fowler yield is based on a semiclassical model of hot electrons emitted over an energetic barrier, with the critical assumption that the kinetic energy *normal* to the barrier must be greater than the barrier height. As depicted in Figure 1(b), for a spherical Fermi surface, this assumption gives rise to a limited escape cone for hot electrons, because the momentum normal to the interface must be larger than a critical value, $p_{crit} = [2m^*(E_F + \phi_b)]^{1/2}$. The escape cone limitation results in zero yield at the threshold photon energy as well as a slow rise with photon energy if the Fermi energy is large compared to the photon energies of interest. This latter condition is true for visible light incident on noble metal emitters; for instance, both silver and gold have a Fermi energy near 5.5 eV (which was the value for E_F used in our calculations).

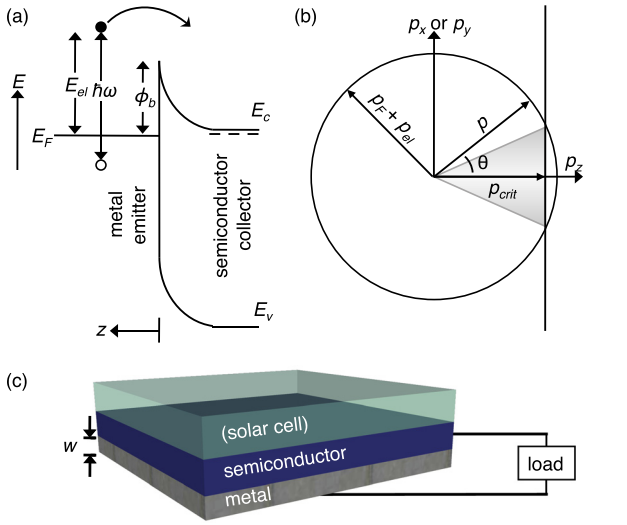

FIG. 1. (a) Internal photoemission band diagram for hot electrons emitted from a metal into an n-type semiconductor. (b) Schematic of isotropic distribution of hot electron momentum on a sphere in momentum space with a limited escape cone. (c) Sketch of a possible energy conversion device layout where light passing through a photovoltaic solar cell and the semiconductor collector is absorbed in the metal emitter.

The collector material can be either an insulator or a semiconductor, and the built-in electric fields of metal-semiconductor Schottky barriers assist in the collection of the emitted hot carriers. In principle, a metal-insulator-metal diode could also be used for energy conversion,[2] but in our calculations the maximum energy-conversion efficiency was found to be equivalent to that of a metal-semiconductor diode (see the supplementary material[27]), so the conceptually and notationally simpler Schottky barrier case will be discussed here, in which the metal is the emitter and the semiconductor is the collector. Considering hot-electron emission, the optimal semiconductor will be a highly doped n-type material, and the Fermi energy in the semiconductor should be nearly equal to the conduction-band energy. Equivalent considerations apply to a p-type semiconductor that would collect hot holes, but here for clarity we consider only the n-type case. To operate in power-generation mode, the diode must be forward-biased (by applying a positive voltage to the metal), in contrast to most internal photoemission detection experiments in which reverse bias aids in extracting the carriers.

The current-voltage characteristics can be determined by considering the reverse photocurrent density due to internal photoemission J_{photo}, the dark forward current density due to thermionic emission from the collector to the emitter J_{dark}, and the properties of the illumination source. The efficiency is given by

$$\begin{aligned} \%\,\text{eff} &= \frac{|J_{photo} + J_{dark}|V}{P_{ill}} \times 100, \\ &= \frac{\left|-\int_0^{\hbar\omega_{\max}} I_{ill}Y(\hbar\omega)(q/\hbar\omega)d(\hbar\omega) + J_{dark}(V)\right|V}{\int_0^{\hbar\omega_{\max}} I_{ill}d(\hbar\omega)} \times 100, \end{aligned} \tag{2}$$

where V is the operating voltage, P_{ill} is the illumination irradiance, I_{ill} is the spectral irradiance, and the integration is performed up to a maximum energy $\hbar\omega_{\max}$. Note that here the yield Y is the external quantum yield, but Y is assumed to be equal to the internal quantum yield under the condition of negligible optical reflection losses. To model the AM1.5 solar spectrum, the spectral irradiance was assumed to be a 5800 K blackbody with a total irradiance of 95 mW cm^{-2}. which provides an easily integratable function that generally matches the shape and irradiance of the AM1.5 spectrum.

The thermionic dark current is given by

$$J_{dark,therm} = A^* T^2 e^{\frac{q(V-\phi_b)}{kT}}, \tag{3}$$

where A* is the Richardson's constant, T is the absolute temperature, and k is Boltzmann's constant. Here, we are assuming that the operating voltage is less than the barrier height but a few times greater than the thermal voltage kT. Though Richardson's constant is given as 120 A cm^{-2} K^{-1}, in our calculations, we generously assumed the more optimistic value of A* ≈ 50 A cm^{-2} K^{-1} which applies for thermionic emission involving a semiconductor like silicon; however, this more optimistic value only results in a maximum of 10% relative efficiency increase relative to the more stringent condition with A* = 120 A cm^{-2} K^{-1}.

Figure 2(a) displays the efficiency for hot carrier internal photoemission assuming the simple Fowler yield based on Eqs. (1)–(3). Because one application of this concept involves capture of sub-bandgap illumination below a traditional photovoltaic cell as shown schematically in Figure 1(c), the efficiency is plotted as a function of maximum photon energy. Hence, the maximum photon energy would be 1.1 eV for a Si solar cell, 3.0 eV for a TiO_2 photoelectrochemical device, or about 4 eV for the entire solar spectrum. The inset shows an example current-voltage behaviour, which has a shape that is similar to a standard pn-junction or Schottky solar cell, but at a much lower operating voltage and current. Figure 2(b) displays the barrier height and voltage at the maximum power point, V_{mpp} for the maximum efficiency values displayed in Figure 2(a). The yield is highest for a small energy barrier, but avoiding the thermionic dark current requires a larger barrier. Specifically, for operation at 1 sun and 300 K, a difference of ~0.7 eV between ϕ_b and V_{mpp} is required to keep the thermionic dark current less than the photocurrent. The thermionic dark current for metal-semiconductor Schottky barrier solar cells can be reduced by introducing a higher barrier for majority carriers, but internal photoemission is entirely a majority-carrier process, so any extra barrier will also reduce the photocurrent.

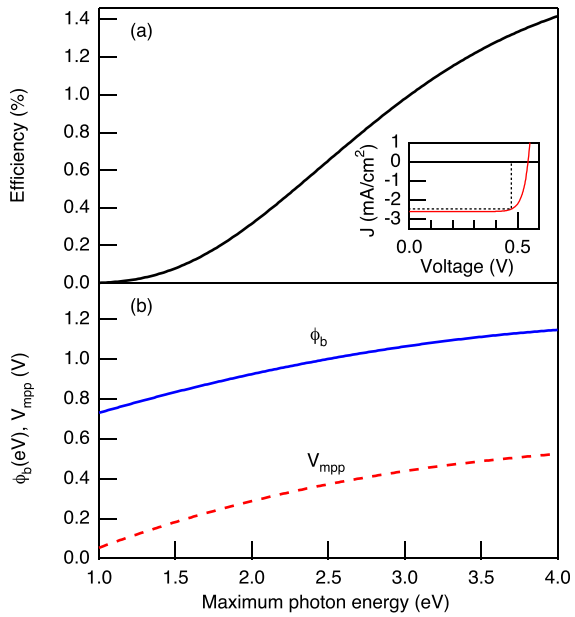

FIG. 2. (a) Solar conversion efficiency for internal photoemission over a metal-semiconductor Schottky barrier based upon the simple Fowler equation. (b) Optimized barrier height and maximum power point voltage (V_{mpp}) used to calculate the curve in (a). Inset: Example current-voltage curve with maximum power shown as the dotted box.

III. THE THREE-STEP MODEL FOR INTERNAL PHOTOEMISSION

Because the simple Fowler equation predicts that the maximum efficiency of an energy-conversion device based on internal photoemission is ~1%, it is useful to analyze the assumptions and mechanisms involved in derivation of the Fowler theory to determine the conditions, if any, that could result in higher efficiencies. The semiclassical model of internal photoemission involves three steps: hot-electron excitation, hot-electron transport to the interfacial barrier, and hot-electron emission over the energetic barrier from the emitter material into the collector material. Although the actual processes of light absorption and excitation of the collective electron cloud are quantum-mechanical phenomena, we assume herein that after light absorption, the "hot electron" behaves as a quasiparticle whose transport can be described semiclassically within a free-electron-like band structure.

Light is absorbed in the metal when the photon's perturbing electric field causes electronic transitions. Consequently, the material response is described macroscopically by a frequency-dependent dielectric constant, ε, determined empirically for bulk materials. Assuming that this local, linear permittivity is a valid description for nanoscale structures such as plasmonic absorbers, Maxwell's equations yield the spectral power absorption as

$$P_{abs} = -\frac{1}{2} Re[-\nabla \cdot \mathrm{S}] = -\frac{1}{2}\omega |E|^2 \mathrm{Im}[\varepsilon] \propto \eta_e, \tag{4}$$

where **S** is the Poynting vector, E is the electric field of the incident electromagnetic wave, and η_e is the hot electron generation rate per length. The spatial distribution of absorbed power is obtained from Eq. (4), and for antenna-like structures, the absorbed power is highest near the surfaces around the midpoint where the highest currents flow. Assuming that the probability is low for an absorbed photon to couple directly to phonons or multiple electron excitations (because many-body excitations are not very probable), the spatial power absorption normalized by the incident power then directly corresponds to the spatial distribution of hot-electron generation. Such calculations are readily performed

using, e.g., full-field finite difference time domain simulations, but the generation profile depends significantly on the geometry of the antenna and system as a whole. Hence, for simplicity, the generation profile was assumed herein to be uniform throughout a film of thickness w, i.e., $\eta_e = 1/w$.

The electron-hole pair excited by light was assumed to have a total energy equal to the photon energy, so the hot electron energy, E_{el}, can range from 0 to $\hbar\omega$. In the simplest approximation, the distribution of energies would be uniform in this range. However, considering the electronic density of states $g(E)$ and nondirect transitions in which momentum can be supplied by surfaces, defects, or phonons, the probability of excitation to a certain energy $E = E_F + E_{el}$ is just the multiplied probability of the existing initial and final states, normalized to the total number of transitions possible

$$P_0(E_{el})dE = \frac{g(E)g(E-\hbar\omega)dE}{\int_{E_F}^{E_F+\hbar\omega} g(E')g(E'-\hbar\omega)dE'}. \tag{5}$$

For a free-electron-like metal with a parabolic band structure at low temperature, such that the tails of the Fermi distribution can be ignored, the hot electron energy distribution becomes

$$P_0(E_{el})dE = \frac{\sqrt{E_F+E_{el}}\sqrt{E_F+E_{el}-\hbar\omega}dE}{\int_{E_F}^{E_F+\hbar\omega} \sqrt{E'}\sqrt{E'-\hbar\omega}dE'} \tag{6}$$

which was used in these calculations. Many metals are free-electron like near the Fermi energy, e.g., for gold the bands with d-orbital character lie about 1.6 eV below the Fermi level, so this approximation is most valid for low photon energy excitation. The relative distribution of hot electrons and hot holes varies depending on the material, and low-lying bands could favor hot holes over hot electrons due to the increased density of states below the Fermi level; modification of the "electron distribution joint density of states" could, in principle, increase (or decrease) the yield and efficiency.[3]

After excitation, the hot electron quasiparticle must move through the material to reach a collecting interface. Because phonon scattering is a quasielastic process, only electron-electron scattering is assumed to cause significant energy loss of the hot electrons. Typically $\sim 1/2$ of the hot electron's energy is lost in an electron-electron scattering event, and the resulting electron can no longer surmount the barrier. The mean free path for electron-electron scattering therefore determines the probability P_{int} that the hot electron will reach the interface, if starting at a depth z at an angle θ away from normal

$$P_{\text{int}}\sin\theta d\theta = \frac{1}{2}\exp\left(-\frac{z}{\lambda_{e-e}(E_{el})\cos\theta}\right)\sin\theta d\theta, \tag{7}$$

where the factor of $1/2$ results from half of the electrons initially travelling away from the interface. A suitable analytical model for the electron-electron scattering mean free path was developed by Quinn and is given as

$$\lambda_{e-e}(E_{el}) = \frac{24a_0\sqrt{\alpha_e r_s/\pi}\left(3E_F/E_{el}^2 + 2/E_{el}\right)}{\tan^{-1}\sqrt{\frac{\pi}{\alpha_e r_s}} + \frac{\sqrt{\alpha_e r_s/\pi}}{1+\alpha_e r_s/\pi}}, \tag{8}$$

where a_0 is the Bohr radius (0.0529 nm), $\alpha_e = (4/(9\pi))^{1/2}$, and r_s is the radius of a sphere equal to the volume of one conduction electron in units of the Bohr radius; for gold $r_s = 3$. The value of $\lambda_{e\text{-}e}$ approximately follows a E_{el}^{-2} behaviour, with some example values being 100 nm at 1 eV to 10 nm at 3.5 eV (a plot of Eq. (8) is included in the supplementary material[27]). Thus, the details of the spatial hot electron generation profile are not critical, because the distances travelled are relatively long compared to the nanoscale dimensions of exemplary plasmonic structures. Though the mean free path can be longer than the characteristic dimension of the metallic nanostructure, the escape cone restriction (vide infra) dictates that, in general, multiple reflections within the metal will occur before the hot electron can be emitted.

When the hot electron encounters the surface and energy barrier, Fowler's theory asserts that the component of kinetic energy normal to the barrier must equal the barrier energy. This requirement is illustrated as the limited momentum escape cone in Figure 1(b), with the maximum angle of approach for which a hot electron can escape given by

$$\cos\theta_{\max} = \frac{p_{crit}}{p} = \sqrt{\frac{E_F+\phi_b}{E_F+E_{el}}} \approx 1 - \frac{E_{el}-\phi_b}{2E_F}, \tag{9}$$

where the approximation holds if ϕ_b, $E_{el} \ll E_F$. This angle defines the maximum angle allowed in Eq. (6). Note that the fraction of hot electrons reflected by the barrier R_{elec} can be written as

$$\begin{aligned} R_{elec} &= 1 - T_{elec} = 1 - \int_0^{\theta_{max}} \sin\theta d\theta, \\ R_{elec} &\approx 1 - \frac{E_{el}-\phi_b}{2E_F}, \end{aligned} \tag{10}$$

where T_{elec} is the transmitted fraction. For large Fermi energies compared to the excitation energy, the reflected fraction is nearly unity.

The internal photoemission yield as a function of energy is obtained by combining the probabilities of absorption, transport to the barrier, and emission over the barrier,

$$Y(\hbar\omega) = \int_{\phi_b}^{\hbar\omega} dE_{el}\int_0^{\theta_{\max}} \sin\theta d\theta \int_0^{\infty} dz P_0(E_{el})P_{\text{int}}(z,\theta,E_{el})\eta_e(z). \tag{11}$$

Under the conditions of $p_{crit} \approx p_F$ so that the escape cone is small, a small absorption length compared to $\lambda_{e\text{-}e}$, and a constant distribution of hot electron energies, the integrals are easily evaluated and result in the Fowler yield, Eq. (1), which is a good approximation for light incident on a bulk slab of metal.

IV. ENHANCEMENTS DUE TO SCATTERING

For thin metal emitters that have a thickness on the order of $\lambda_{e\text{-}e}$, the yield can be enhanced significantly due to

Lambertian reflections at the interfaces. Electron-phonon scattering with a mean free path $\lambda_{e\text{-}p} \sim 20\,\text{nm}$ (used in the calculations here) can additionally enhance the yield, because the hot electron momentum can be redirected into the escape cone with little loss of energy in the quasi-elastic collisions. Again considering the case of $p_{crit} \approx p_F$, Dalal[22] has derived an enhanced yield expression that takes into account both phonon and back-surface scattering. In this model (see Ref. 22 for more details), the angular integral of P_{int} is replaced with a more detailed function $q(z)$ due to a sum over multiple reflections at various scattering angles, producing the following expression for enhanced yield:

$$
\begin{aligned}
Y_{enh}(\hbar\omega) &= \int_{\phi_b}^{\hbar\omega} dE_{el} \int_0^{\infty} dz P_0(E_{el}) q(E_{el}, z) \eta_e(z), \\
q(E_{el}, z) &= A_w e^{\mu z} + B_w e^{-\mu z}, \\
A_w &= e^{-2\mu w} B_w, \\
B_w &= \frac{1 - R_{elec}}{(1 - R_{elec})(1 + e^{-2\mu w}) + \left(1 + \dfrac{\lambda_{e-e}}{\lambda_{e-p}}\right)^{-1/2} (1 + R_{elec})(1 - e^{-2\mu w})}, \\
\mu &= \sqrt{(\lambda_{e-e}^{-1} + \lambda_{e-p}^{-1})^2 - \lambda_{e-p}^{-1}(\lambda_{e-e}^{-1} + \lambda_{e-p}^{-1})},
\end{aligned}
\tag{12}
$$

where w is the metal thickness in the z direction. Relative to Fowler's treatment, phonon scattering effectively boosts the yield by a factor $(\lambda_{e\text{-}e}/\lambda_{e\text{-}p})^{1/2}$ for emission from a bulk emitter, and the yield increases strongly with reduced thickness of the metal; a plot of the thickness effect is included in the supplementary material.[27]

For extremely thin films, Y_{enh} diverges because the assumption of $R_{elec} \sim 1$ that was used to derive Eq. (12) is no longer valid. Instead, for a best-case yield that may be appropriate to describe the behaviour of very thin and rough films in which the escape cone restriction is relaxed, the condition $R_{elec} \sim 0$ applies. This condition can be met by modifying Eq. (6) to set $\theta_{max} = \pi/2$ and to include one specular reflection off the back surface. In this situation, phonon scattering is irrelevant if $w < \lambda_{e\text{-}p}$. In the limiting case of $\lambda_{e\text{-}e} \gg w$, all of the hot electrons with sufficient energy will be emitted, and in the best-case scenario $P_{int} = 1$. For this hypothetical case, with no escape-cone limitation, the yield is only limited by the distribution of hot electron energies; the analyses in Refs. 2 and 3 correspond to this extremely thin film assumption.

V. THEORETICAL EFFICIENCIES

Based on the equations for yield outlined in Secs. III and IV, the efficiency given by Eq. (1) can be numerically evaluated for a variety of conditions and assumptions. Figure 3 shows the optimized efficiency as a function of maximum photon energy, assuming that the incident light is completely and uniformly absorbed over the film thickness with no reflection losses. Figure 3 includes (on a logarithmic scale) the result from Figure 1(a) based on the Fowler yield but also shows results for a 100 nm metal film ($E_F = 5.5\,\text{eV}$) at 300 K, a 20 nm film at 300 K, a 20 nm film at 300 K for which $R_{elec} = 0$, and a 20 nm film at 77 K, as well as the best-case scenario at both 300 and 77 K for which the hot electron mean free path is much longer than the film thickness. Note that when the momentum escape cone restriction is included, with either finite film thickness, the calculated efficiency is much lower than the best-case scenario in which the escape cone restriction is not explicitly included in the analysis.

The 100 nm and 20 nm cases at 300 K show lower efficiency than the simple estimate from the Fowler equation, due to the inclusion of a finite electron mean free path, which affects light absorbed deeply in the metal. In contrast, the Fowler case assumed absorption at the surface. Operation of such devices at lower temperature enhances the efficiency, because the dark current from thermionic emission is lowered significantly as the temperature decreases. Clearly, the efficiency reaches values significantly in excess of 1% only if the escape cone restriction is lifted in the best-case scenario and if photon energies above 1.5 eV are included.

VI. DISCUSSION

In this semiclassical model of hot electron internal photoemission, the energy-conversion efficiency is low for two

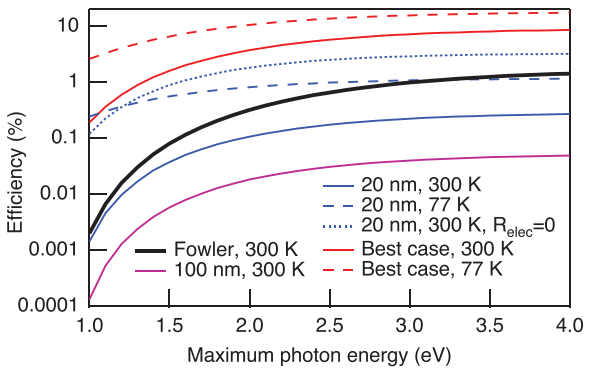

FIG. 3. Solar conversion efficiency for IPE considering a 5800 K blackbody spectrum up to a given maximum photon energy fully absorbed in an Au-like metal considering different film thicknesses (colors), operating temperatures (dashed lines), and escape cone limitations (dotted line). The simple Fowler case from Fig. 1 is included as the bold black line, and "best case" represents a very long hot electron mean free path compared to the dimensions of the structure itself.

primary reasons. First, the diode must be operated in forward bias to capture the reverse photocurrent, so the thermionic current of electrons flowing from the collector to the emitter strongly reduces the net current. Second, each photon creates a hot electron and a hot hole, and the hot electron energy can easily be less than the photon energy. In contrast to a semiconductor photovoltaic device in which the internal energy of the minority carriers is nearly equal to the bandgap, the internal energy of the hot electrons involved here is distributed from zero to the photon energy.

Although the most optimistic assumptions were used in most cases, the results could be modified by explicit consideration of some other effects. The band structure of real materials can change the distribution of hot electron (and hot hole) energy, so the transition probabilities linking initial and final electronic band states should be calculated to determine the excitation probabilities as a function of both the hot electron/hole energy and momentum. An optimized band structure or device layout may allow higher efficiency than that calculated herein. We have used reasonable numbers for a Au/n-Si junction, but the efficiency estimates here should be applicable to a wide range of metal/semiconductor materials because the hot electron mean free paths do not vary wildly for various metals. Also, the efficiencies presented here are not true detailed-balance efficiencies, because no re-radiation of light was considered. Considering optical reflection and photon emission would further lower the efficiencies.

Another limitation exists due to the requirement of critical momentum normal to the interface, which leads to a small escape cone for hot electrons having an energy just larger than the barrier energy. For an interface that is rough on the scale of the electron wavelength, this classical restriction may be relaxed. Indeed, some vacuum photoemission experiments have seen anomalously high yields from nanoparticles,[20] with a variety of explanations involving geometry, escape cone relaxation, and surface chemistry modification.[28–30] In theory, the quantum mechanical details of plasmon-mediated hot carrier production may introduce a momentum-polarization correlation. Qualitatively, this coupling may enhance photocurrent along certain geometry-dependent directions at specific polarizations. This coupling tends to relax the escape cone considerations, by allowing final electron momenta that are usually disallowed by regular IPE processes. As a result, the yield may be increased up to the $R_{elec} = 0$ case. However, simply relaxing the escape cone restriction without addressing the dark current and hot electron energy distribution limitations still results in energy-conversion efficiencies of a few percent at best (Fig. 3).

Because conventional photovoltaic cells do not absorb light below the bandgap energy, exploitation of IPE might be a potentially interesting method for capturing the otherwise unutilized part of the solar spectrum by placing the device behind a solar cell. In this arrangement, use of the metal/semiconductor device would be analogous to placing another, low band gap, semiconductor absorber and associated metallurgical junction in the optical path. The system instead relies on optical absorption and charge carrier excitation in the metal portion of the metal/semiconductor system (with a large band gap semiconductor, in principle), to produce the additional current and thus augment the device efficiency. As displayed in Figure 3, however, the yield and efficiency increase strongly as the photon energy is increased, and IPE is particularly inefficient for a spectrum that only includes energies below 1–2 eV. Hence, such an approach would be more appropriate for larger-bandgap devices that normally only absorb ultraviolet light, such as a TiO_2-based photoelectrochemical system than for an additional absorber approach to a conventional solar cell arrangement.

The metallic emitter was implicitly assumed to be a nanostructure that possessed plasmonic resonances so as to provide high absorption in a very thin structure[18] and additionally to take advantage of the enhancements in scattering. The spatial distribution of hot electron generation may vary for such nanostructures, likely depending on the position of absorption based on the Poynting vector (Eq. (4)). For example, a dipole antenna has the highest current and dissipation of energy near its center. The hot electrons may possibly instead be generated near areas of high field enhancement.[12] Regardless, for these relatively low-energy hot electrons, the electron-electron scattering mean free path is on the same order as a plasmonic nanoparticle's dimensions, so the specific location of hot electron generation is of minor importance. The hot electron's initial momentum is, however, very important for the yield, as particles with a momentum vector inside the escape cone have a much higher probability of escape than those with momentum vectors outside the escape cone.

The efficiencies presented here are somewhat lower than some previous published calculations. Wang and Melosh[2] considered power conversion using Kretschmann coupling to surface plasmon polaritons in a symmetric metal-insulator-metal geometry and obtained a calculated maximum efficiency of 2.7%. Their calculation assumed no escape cone restriction, no carrier reflections, a uniform energy distribution of excited carriers, and an energy-independent $\lambda_{e\text{-}e} = 56$ nm. The result is on the same order as that calculated here including, however, the assumption (for which the justification is unclear) of no escape cone restriction; similarly, White and Catchpole calculated a maximum efficiency of 8% by assuming that all hot electrons with sufficient energy in a perfect absorber were emitted.[3] Although it is tempting to assume that for nanostructured metallic absorbers the hot electron mean free path will be sufficiently longer than the device dimension and thus that the momentum escape cone restriction can be neglected,[2,3] we have shown herein that even a small non-zero thickness (of 20 nm) of metal lowers the efficiency from 8% to 0.25% (c.f. Figure 3 blue solid line). Schmidt *et al.* postulated energy-conversion efficiencies up to 10% even with the escape cone restriction;[31] however, the thermionic dark current was neglected in their approach and their treatment additionally incorrectly used the barrier height as the operating voltage in Eq. (2).

Finally, some deleterious effects were not included in our model. Scattering of hot electrons back into the emitter from the collector will reduce the yield, especially for diodes operated in forward bias with a weak electric field in the collector. Similarly, internal photoemission from the nominal collector to the emitter reduces the net photocurrent. Energetic losses due to phonon scattering also could

somewhat reduce the yield. Emission of hot holes into the same material could take place if the collector is a low-bandgap semiconductor, reducing the yield. Last, interfacial and bulk defects present in real materials will lower the hot electron mean free paths and collection efficiency, decreasing the device efficiency. In principle, this metal-emitter junction could be placed at the back of a photovoltaic device, but the details of device integration and effects on the photovoltaic efficiency are beyond the scope of this work.

VII. CONCLUSIONS

The process of internal photoemission in which the absorbing material is a metal rather than a semiconductor was evaluated as a candidate for utilization in solar energy-conversion devices. The semiclassical three-step model of internal photoemission for hot electrons over an energetic Schottky barrier was reviewed, and the energy-conversion efficiency was calculated considering the IPE photocurrent produced by complete absorption of a 5800 K blackbody spectrum in a nanoscale metal and the thermionic emission dark current as a function of voltage. The optimum efficiency values were found to be $\sim 1\%$ for room-temperature operation with a metal similar to Au or Ag. The efficiency could approach 10% if the escape cone restriction is removed, the mean free path of hot electrons is very long compared to the metal dimensions, and the illumination spectrum includes visible and ultraviolet light, in which case the efficiency is still limited by the thermionic dark current as well as by the distribution of hot electron energies (without modifying the metal's joint density of states). We have shown herein that considering the momentum escape cone imposes a significant limit on efficiency even for nanostructures. Additional work to determine the applicability of this admittedly semiclassical model would be useful because the normal momentum requirement might be relaxed when considering quantum effects or surface chemistry. Alternatively, a device geometry in which light capture is decoupled from hot electron-hole generation in a metal bi-layer could possibly reduce the emitter thickness to the nm-size thickness required to justify neglecting the escape cone restriction.

ACKNOWLEDGMENTS

This material is based upon work performed by the Joint Center for Artificial Photosynthesis, a DOE Energy Innovation Hub, supported through the Office of Science of the U.S. Department of Energy under Award No. DE-SC0004993. P.N. is supported by a National Science Foundation Graduate Research Fellowship and by the Resnick Sustainability Institute.

[1]W. Shockley and H. J. Queisser, J. Appl. Phys. **32**, 510 (1961).
[2]F. Wang and N. A. Melosh, Nano Lett. **11**, 5426–5430 (2011).
[3]T. P. White and K. R. Catchpole, Appl. Phys. Lett. **101**, 073905 (2012).
[4]R. T. Ross and A. J. Nozik, J. Appl. Phys. **53**, 3813–3818 (1982).
[5]M. W. Knight, H. Sobhani, P. Nordlander, and N. J. Halas, Science **332**, 702–704 (2011).
[6]Z. Fang, Z. Liu, Y. Wang, P. M. Ajayan, P. Nordlander, and N. J. Halas, Nano Lett. **12**, 3808–3813 (2012).
[7]S. Mubeen, G. Hernandez-Sosa, D. Moses, J. Lee, and M. Moskovits, Nano Lett. **11**, 5548–5552 (2011).
[8]Y. K. Lee, C. H. Jung, J. Park, H. Seo, G. A. Somorjai, and J. Y. Park, Nano Lett. **11**, 4251–4255 (2011).
[9]I. Goykhman, B. Desiatov, J. Khurgin, J. Shappir, and U. Levy, Nano Lett. **11**, 2219–2224 (2011).
[10]A. Akbari, R. N. Tait, and P. Berini, Opt Express **18**, 8505–8514 (2010).
[11]Y. Nishijima, K. Ueno, Y. Yokota, K. Murakoshi, and H. Misawa, J. Phys. Chem. Lett. **1**, 2031–2036 (2010).
[12]E. Kazuma, N. Sakai, and T. Tatsuma, Chem. Commun. **47**, 5777 (2011).
[13]Y. Tian and T. Tatsuma, J. Am. Chem. Soc. **127**, 7632–7637 (2005).
[14]S. Linic, P. Christopher, and D. B. Ingram, Nature Mater. **10**, 911–921 (2011).
[15]X. Wu, E. S. Thrall, H. Liu, M. Steigerwald, and L. Brus, J. Phys. Chem. C **114**, 12896–12899 (2010).
[16]S. Mubeen, J. Lee, N. Singh, S. Krämer, G. D. Stucky, and M. Moskovits, Nat. Nanotechnol. **8**, 247–251 (2013).
[17]A. Polman and H. A. Atwater, Nature Mater. **11**, 174–177 (2012).
[18]K. Aydin, V. E. Ferry, R. M. Briggs, and H. A. Atwater, Nat. Commun. **2**, 517 (2011).
[19]M. W. Knight, Y. Wang, A. S. Urban, A. Sobhani, B. Y. Zheng, P. Nordlander, and N. J. Halas, Nano Lett. **13**, 1687–1692 (2013).
[20]A. Schmidt-Ott, P. Schurtenberger, and H. C. Siegmann, Phys. Rev. Lett. **45**, 1284–1287 (1980).
[21]E. O. Kane, Phys. Rev. **147**, 335 (1966).
[22]V. L. Dalal, J. Appl. Phys. **42**, 2274 (1971).
[23]R. H. Fowler, Phys. Rev. **38**, 45 (1931).
[24]V. E. Vickers, Appl. Opt. **10**, 2190–2192 (1971).
[25]D. Kovacs, J. Winter, S. Meyer, A. Wucher, and D. Diesing, Phys. Rev. B **76**, 235408 (2007).
[26]V. V. Afanas'ev, *Internal Photoemission Spectroscopy: Principles and Applications* (Elsevier, Amsterdam, 2008).
[27]See supplementary material at http://dx.doi.org/10.1063/1.4870040 for the efficiency calculation of a metal-insulator-metal diode geometry and additional plots visualizing equations.
[28]U. Muller, H. Burtscher, and A. Schmidt-Ott, Phys. Rev. B **38**, 7814–7816 (1988).
[29]Q. Y. Chen and C. W. Bates, Phys. Rev. Lett. **57**, 2737–2740 (1986).
[30]G. Faraci, A. R. Pennisi, and G. Margaritondo, Phys. Rev. B **40**, 4209–4211 (1989).
[31]M. Schmidt, M. Brauer, J. Bannach, and H. Flietner, *Proceedings of the 12th European Photovoltaic Solar Energy Conference*, 1994, pp. 1–5.